Journal of Harbin Engineering University
ISSN: 1006-7043

Vol 44 No. 11
November 2023

Review of Overheat-Preventing Knee Motion in Color Tracking Humanoid Biomechanics based on Gyroscope Sensor

[1]Ridwan Wicaksono, [2]Wahyu Dewanto
[1] [2] Electrical and Information Engineering Department,
Engineering Faculty, Universitas Gadjah Mada, Yogyakarta, Indonesia

Abstract— Overheat-preventing motion in color-tracking humanoid biomechanics has been evaluated based on a gyroscope sensor. To achieve stability, the angular degree of the hip-knee-ankle servos was defined using feedback error data from gyroscope signals. The gyroscope sensor was placed on the humanoid structure's center of mass (COM). A camera was used to identify the anticipated color using the look-up table approach and to determine the image's plane axis's central x Cx and central y Cy using the Region Grow algorithm. The bounding box technique determined the position of the microcontroller's central xy Cxy which was used as input for the neck and waist servos to face the color location. The purpose of this research is to offer consistent walking motion toward the intended color while preventing overheating, particularly in knee actuators. To verify robot stability, two experiments were planned: static and dynamic balance. The studies in static balancing were carried out by tilting the robot toward the y-axis (pitch), which caused the robot to fall. Meanwhile, the dynamic balancing was evaluated based on cross-correlation and autocorrelation of the gyroscope signal. The walking motion is steady in dynamic balancing, but the gyroscope output creates a periodic signal. As a means of evaluating stability, the time-step and lag of gyroscope data were chosen. The temperature of the knee servos was measured under overheat protection at 55°C and compared to the traditional and new methods. Finally, the overheat-preventing walking motion reduces the risk of overheating actuators, which results in a low-temperature increase on the knee servos.

Index Terms— Gyroscope, color tracking, overheat servo, walking motion, humanoid biomechanics*.*

I. INTRODUCTION

A focus area in robotics appears to be extremely viable for academic students, industrials, and robot enthusiasts to explore [1]. As a first step, we are considering using robotics as an instructional approach to integrating hardware, software, and communication technologies in a senior-year course where students have already taken Microcontrollers, Sensors and Transducers, Kinematics, Dynamics, and Machine Design [2], [3]. Bioloid robots are mostly used for amusement and teaching. Stability in reaching certain poses, such as walking, standing, kicking, turning, sitting, rotating, evolving, turning, and alerting, is one of the robot parts examined. The geometrical Analysis Technique (GAT) aids in the design of movement conditions in humanoid robots [4]. In addition, experiments on the integration of image processing science with robot step-motion motions have been conducted [5]. Robots, for example, are programmed to follow specific colors and even manage security systems. However, specified motion parameter values may not always ensure that the robot properly follows the desired color due to instability motion.

Regarding the instability problem, Hemami et al. investigated the static stability of an inverted pendulum, considering feedback techniques for robot-motor control to balance the robot [6]. The potential energy calculation determines the requirement for static stability, which is dependent on the robot's physical factors such as height and foot length. Vukobratovic et al. proposed the Zero Moment Point (ZMP) as a biped robot stability-measurement criterion [7]. Gyroscopes are utilized in both practical applications like navigation and location, as well as basic physics [8], [9]. Nuclear magnetic resonance (NMR) gyroscopes and spin exchange relaxation-free (SERF) gyroscopes are two actively developing nuclear-spin gyroscope designs [10]. To precisely analyze the motion effect, a gyroscope sensor is preferred. For example, after 10 minutes of driving, a combination of a MEMS gyroscope and wheel speed sensors produced a remarkable accuracy of 30 m [11]. Besides, a gyroscope sensor feedback-control system is utilized to govern the robot's stability by adjusting the ankle torque as a function of the humanoid robot's rotational velocity about the robot's toe [12]. However, the integration gyroscope into camera-based color-tracking humanoid robots is still challenging.

Another backward of low-torque humanoid actuators is overheating while dealing with heavy loads [13]. A color-tracking humanoid robot emulated a human position in real time but did not offer servo temperature data [14]. A study

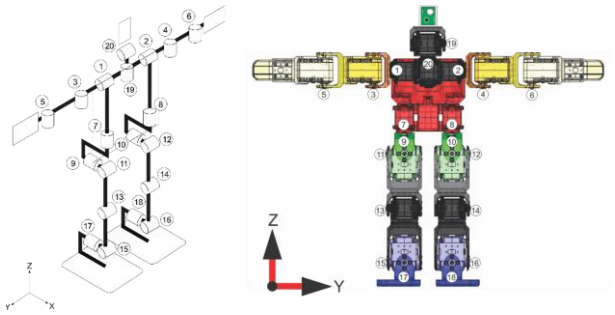

Figure 1 The mechanical structure of humanoid biomechanics.

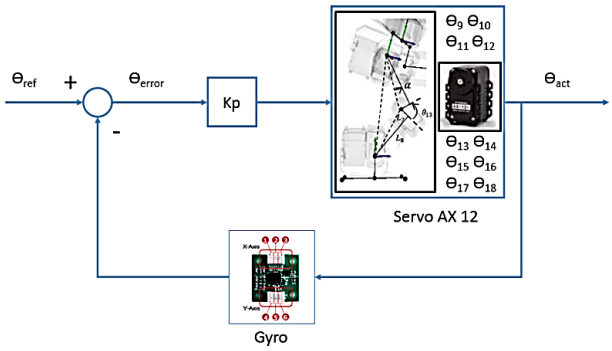

Figure 2 Block diagram of the robot leg system based on gyroscope sensor.

employed interpolation among optimum angles to construct continuous angle trajectories with a NAO humanoid robot, with the findings confirming the efficacy of the suggested technique for dynamic walking [15]. Another study examines the multi-axis force-torque sensor utilized in today's cutting-edge humanoid robots in terms of biped walking, zero-moment point, and ground response force [16]. Even though overheating problems lead servos to explode, neither article covers actuator heat analysis. Due to cost constraints, optimizing an actuator's heat in dynamic motion is essential.

This study intends to develop techniques for an overheat-preventing motion of humanoid robots for color tracking based on gyroscope sensor. Physical experiments are evaluated to analyze the robot's step motion. The humanoid is pushed with a constant force, and the robot's dynamics are monitored and modeled using a simple constant-length inverted pendulum. The feedback control system built into the robot is another consideration. The feedback mechanism is provided by two gyro sensors (pitch and roll), which are used for robot-motion control based on the created model. Technically, once the parameters are known and the robot is stable in attaining a static position, the robot is supposed to perform optimally in dynamic functions. As an evaluation assessment, swinging and heat analysis are provided.

II. METHOD

A. Mechanical structure

The mechanical structure of a humanoid robot is shown in **Figure 1**. A humanoid robot's mechanical construction is intended to resemble the physical look and movement capabilities of a human person and consist of numerous components and subsystems, for instance, servos such as actuators, sensors, and microprocessor. To accomplish robot balance, the angular velocity is supplied back for control of the knee-motor angle. The key focus of this research is the generation of the mechanical trajectory of the knee step motion of the bipedal model.

B. Electronics

1) Gyroscope sensor

Figure 2 depicts the block diagram of the robot leg system based on the gyroscope sensor. A gyro sensor can be inserted to assess the stability of the standby posture. The experiment diverts the robot rotation to the y-axis so that the gyro pitch data changes. A variable is required to establish the standby state, where the value of pitch dataD_p and roll dataD_r are near 258. Due to fluctuation in gyroscope data, the average pitch and roll data were determined using *N* = 30 samples. Both static pitch dataD_{pc} roll dataD_{rc} were acquired at idle and balanced conditions. The static roll dataD_{pc} were defined by

$$D_{pc} = \frac{D_{pc} + \sum_{n=1}^{N} D_p}{N} \quad (1)$$

Meanwhile, the static roll dataD_{pc} were defined by

$$D_{rc} = \frac{D_{rc} + \sum_{n=1}^{N} D_r}{N} \quad (2)$$

2) Color-tracking sensor

The reading and processing speed of HaViMo 2.0 is between 10 and 11 Hz which is enough for low-scaled image processing based on the look-up table (LUT) method, as shown in **Figure 3.a**. Due to high compatibility, the HaViMo 2.0 camera was implemented to detect certain colors and was plugged into the CM530 microcontroller. The expected color that the robot pursues based on the bounding-box algorithm is shown in **Figure 3.b**. In HaViMo 2.0, the Region Grow algorithm generates C_x and C_y image's plane axis of the line location concerning the camera sensor as shown in **Figure 3.c**, defined by

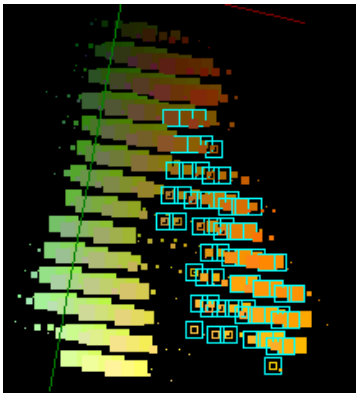

Figure 3.a Look-up table color selection

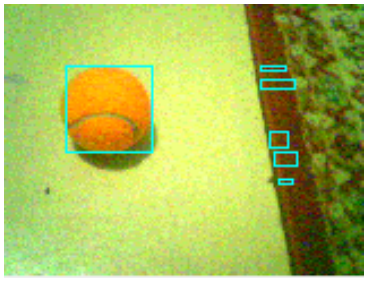

Figure 3.b Bounding-box identification

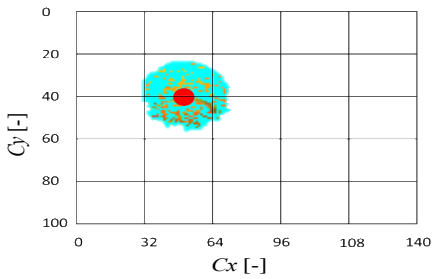

Figure 3.c Position identification

$$C_{xy} = \frac{Cxy_{max} - Cxy_{min}}{2} \qquad (3)$$

Two variables were initialized to define the position of the tracked color data which were a center position of pitch-feedback *FBBalCenter* and roll-feedback *RLBalCenter*. Let's say the center position of C_{xy} (red color in Figure 3.c) is between 40 – 60 on the C_y axis, and between 64 – 96 on the C_x axis. In the case of *FBBalCenter* = 0, no change in C_x data. Also, in the case of *RLBalCenter* = 0, no change in C_y data. The position of C_{xy} influenced the degree of neck and hip actuators to face the robot towards the tracked color, until the offset of *FBBalCenter* and *RLBalCenter* equal to 0.

3) Temperature sensor

The temperature of the knee actuator is the fundamental restriction in a humanoid robot and is cited as a significant evaluation. When a large torque load was applied to the knee actuators, they became heated. Temperature monitoring on the knee actuators is used as overcurrent protection activation when considering overheating protection. The low-torque AX12 servo, being the principal actuator, is susceptible to damage when the temperature exceeds 60°C. Overheat protection was set to 55°C on each knee actuator to minimize the late reaction of current flow that happens when a servo burns out.

C. Walking trajectory

Figure 4.a shows the color tracking flowchart. The robot starts by performing the initial function, which regulates the biomechanics body in a standing position. Second, the camera function is performed by snapping pictures. Third, the picture data is scanned using the lookup table (LUT) approach to match the intended color data. After detecting the intended color, the bounding box algorithm is run. The biomechanics will move until the intended color position is in the center of the coordinate axis. Finally, the robot walks to come closer to the desired hue.

The biomechanics' walking trajectory was influenced by three groups of actuators, which were hip, knee, and ankle servo. **Figures 4.b** and **Figure 4.c** show the walking step-motion illustrations of the backside and from the side of the humanoid biomechanics, respectively. The walking step-motion consists of six steps: (1) shifting the center of mass (COM) at point (0,0) to the pedestal foot (0, Δy) by turning the ankle servo (2) shifting COM at point (0, Δy) to (Δx, Δy) by turning the hip servo (3) raising one sole foot by turning the knee servo, (4) put the sole foot forward, (5) shifting the center of mass (COM) and (6) returning the COM at point (0,0).

III. EXPERIMENTS

Figure 5.a shows an overview of static experiments. The experimental conditions were performed by tilting the humanoid biomechanics towards the y-axis (pitch) since variations in angular velocity in the y-axis have the greatest influence on the static biomechanics' balance in the standby position. The change in angular velocity in the roll data (rotation about the x-axis) has no substantial effect on the standby position's balance.

Figure 5.b depicts an overview of dynamic experiments. In dynamic functions, Roboplus software was used to configure data in humanoid biomechanics step-motion. Parameters were determined in this program to enter data into the robot actuators. Servo degree, repeat duration, speed rate, control inertia force, and joint softness are the most significant factors in determining the trajectory of motion.

IV. RESULTS AND DISCUSSION

A. Static Balancing

In the case of the without gyroscope, the robot swings more than when it is installed. The robot is resisted from falling when the angle of deviation is more than 20^o or less than -20^o. When the angle of deviation is between -15^o and 15^o, the robot is damped to an equilibrium position. There

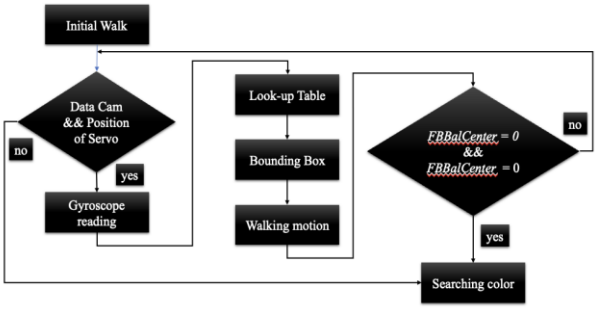

Figure 4.a Color tracking flowchart.

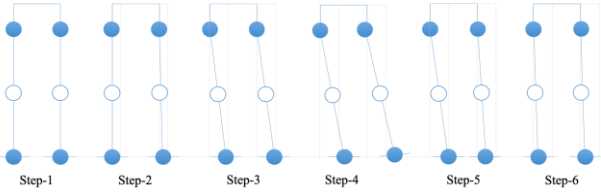

Figure 4.b Illustration of the backside of the robot (change in roll axis).

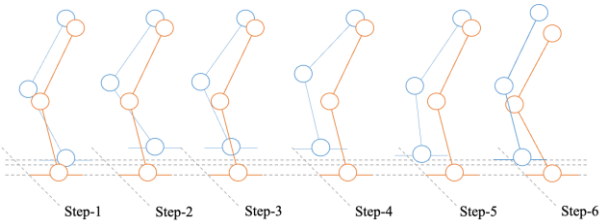

Figure 4.c Illustration from the side of the robot (changes to the pitch axis).

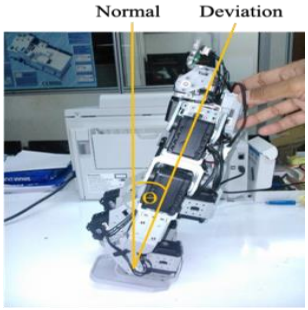

Figure 5.a Static balancing

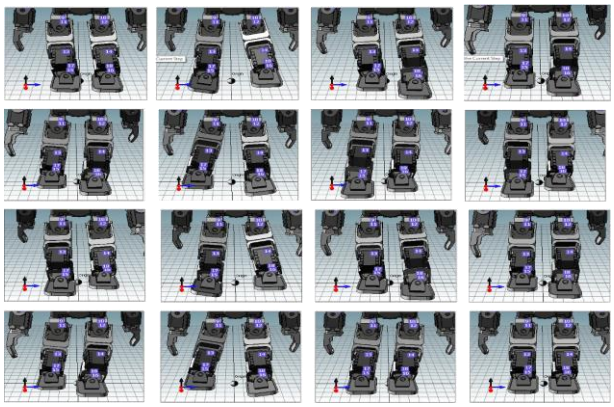

Figure 5.b Dynamic balancing

are swings before the robot achieves a steady state. The gyroscope must be present and functioning to offer feedback. The difference between D_p-D_{pc} or D_r-D_{rc} values provide the degree of servos that impact pitch and roll balancing. However, before entering the servo, the value is multiplied by the proportional constant (*PC*). Each servo has a unique *PC* value. After multiplying by the *PC* value, the offset value of the joints (servo) affecting pitch and roll balancing is obtained. When the robot is tested with a gyroscope fitted, the number of swings required to attain stability decreases. The statistics in **Table 1** demonstrate static balance experiments.

Table 1 Static-balancing experiments.

STATE	ANGLE	CONVENTIONAL METHOD	PROPOSED METHOD
1	-25°	Fall	2 times swinging
2	-20°	Fall	2 times swinging
3	-15°	4 times swinging	1 time swinging
4	-10°	3 times swinging	1 time swinging
5	-5°	2 times swinging	Dampened
6	0°	-	-
7	5°	2 times swinging	Dampened
8	10°	3 times swinging	1 time swinging
9	15°	4 times swinging	1 time swinging
10	20°	Fall	2 times swinging
11	25°	Fall	2 times swinging
12	30°	Fall	3 times swinging

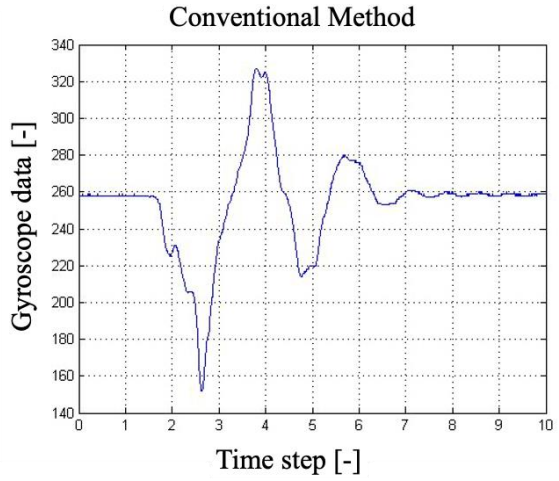

Figure 6.a Gyroscope time-step evaluation of conventional knee motion.

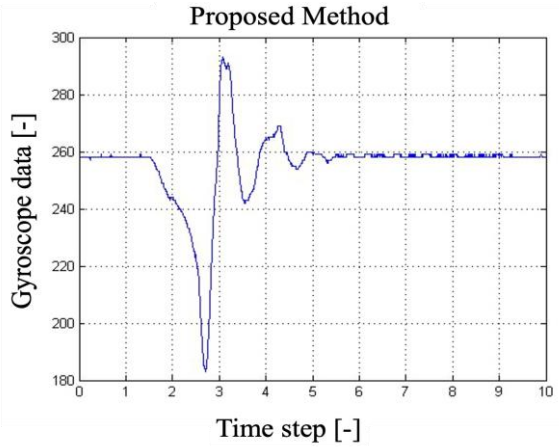

Figure 6.b Gyroscope time-step evaluation of overheat-preventing knee motion.

According to the test findings, the robot with a gyroscope returns to balance and stabilizes with less lag time than the robot without a gyroscope. The system with gyroscope feedback has a higher snapshot in the cross-correlation snapshot picture than the system without gyroscope feedback. This is due to the proportional constant (*PC*), which gives the extra offset in servos 11, 12, 13, 14, 15, and 16 for mistakes caused by changes in pitch angular velocity and servos 9, 10, 17, and 18 for errors caused by changes in roll angular velocity. The results discovered that the gyroscope sensor may be utilized to keep the robot stable when it is stationary, as shown in **Figures 6.a** and **Figure 6.b**. The lag range of the gyro signal of the robot without feedback is greater than that of the

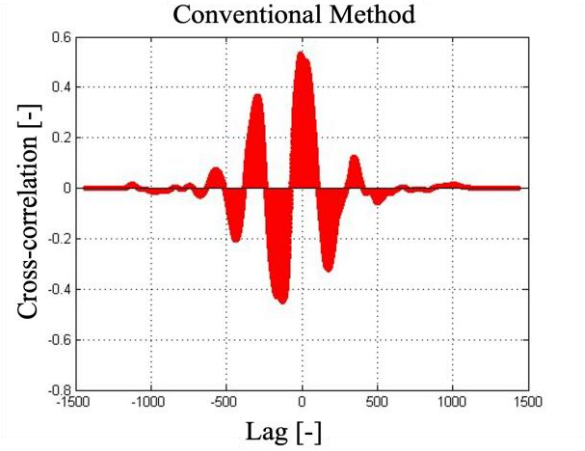

Figure 7.a Lag of conventional knee motion.

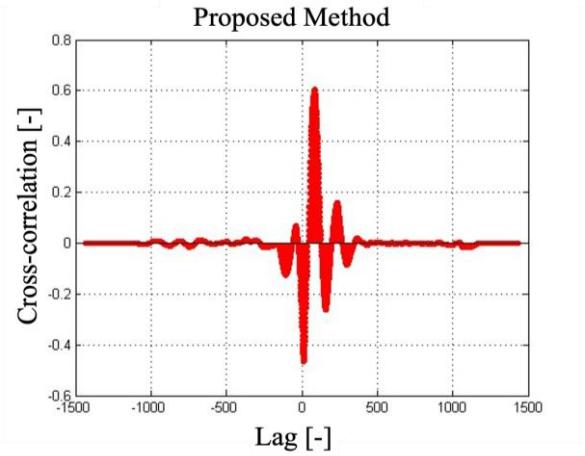

Figure 7.b Lag of overheat-preventing knee motion.

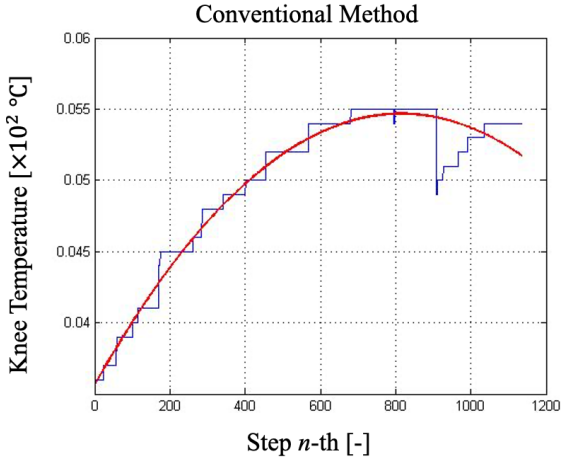

Figure 8.a Temperature of conventional knee motion.

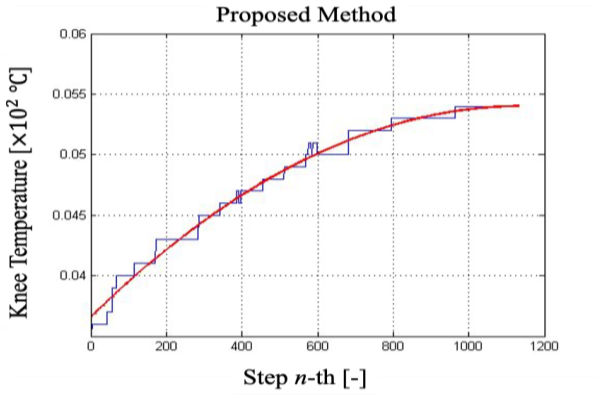

Figure 8.b Temperature of overheat-preventing knee motion.

robot with gyro feedback, according to the cross-correlated technique. The quicker the steady state, the narrower the lag range.

B. Dynamic Balancing

A periodic shift in angular velocity occurs when the robot walks in a balanced way at a constant speed. The pitch and roll readings from the gyroscope show the angular velocity. **Figures 7.a** and **Figures 7.b** show graphs of pitch-periodicity data from robot motion against lag. autocorrelation may be used to determine if data is periodic or not. On the auto-correlation graph, the features of a periodic signal are the larger the lag, the value of the auto-correlation snapshot is closer to 0. The auto-correlation value is 0 when the latency is equal to *N*. Moreover, both figures illustrate the results of the cross-correlation of the gyroscope output signal with the signal itself. Based on observations, the servo pairs that have a substantial influence on the movement process and the servo with the greatest angle data changes are servo 11-12, 15-16, and 13-14, respectively. The three servo pairs change a lot of data with a rather abrupt transition. Based on hip-knee-ankle servo observations, the knee servos, servo numbers 13 and 14, were prioritized for heat investigation so that the servo does not overheat.

C. Temperature investigation

The key finding is the inspection of the temperature sensor on the knee dynamixel actuators, ID 13 and 14. This knee servo is subjected to the highest strain and frequently suffers substantial fluctuations in angle data. Running the robot for 8 seconds times 20 seconds is 160 seconds of continuous data collecting. The quadratic trend estimation method is used to do a trend approach based on this data. A red line representing the trend of the voltage drop may be generated using this approach. The 56-step robot movement exhibits a faster drop based on the observed pictures. This signifies that the exponential power value is higher, resulting in a speedier transition. The movement of the 24-step biomechanics has a slower transition graph. As

a result, the exponential value is lower. The trend of the two plots shows that the more steps there are, the faster the voltage drops.

Figures 8.a and **Figures 8.b** show the temperature comparison of conventional and overheat-preventing knee motion, respectively. The temperature on servos 13 and 14 were examined using overheat protection. Both servos have a starting temperature of 32°C. Both statistics demonstrate that the temperature rises as the robot moves. For safety reasons, the researchers limit the servo temperature to 55°C. If the temperature rises over 70°, the motor in the servo burns out, rendering the servo inoperable. When the servo reaches 55°C, the servo indication light illuminates, but the servo is not triggered. Running the robot for 8 seconds times 20 seconds is 160 seconds of continuous data collecting.

Figure 8.a shows that the temperature has dropped because the servo activates the overheat protection. By completing the 16th biomechanics motion test, the robot was shut off for a brief while before being retested. While retested, the findings reveal that it is still near the same thing. The temperature rise exceeds the 24-step biomechanics. In the 24-step biomechanics motion test, the transition is slower, indicating that the exponential magnitude of the temperature rise is less. The +600th data were compared with a temperature value of +50°C. The servo temperature remained below 55°C until the test was finished with T = 160 seconds and 1135 data points. According to the test results, overheat-preventing knee motion minimizes the danger of overheating actuators resulting in a low-temperature increase.

The test findings show that the biomechanics movement with 56 steps has a strong exponential trend, indicating that the transition is faster. The servo temperature was already close to 54°C at the 600th data point. The servo is near to the maximum temperature limit at data to +700, therefore at data to +900, the servo becomes inactive.

V. Conclusion

A gyroscope sensor is successfully implemented to create overheat-preventing motion in color-tracking humanoid biomechanics. The angular degree of the hip-knee-ankle servos was designed utilizing feedback error data from gyroscope signals to ensure stability. To do step-motion testing, the biomechanics must be moved in three stages: stationary to motion, motion to motion, and motion to stationary. When the position is static, the employment of the gyroscope sensor accelerates the biomechanics' position balance in case the robot is in motion to rest or in case the robot picks up unwanted momentum from outside. The employment of gyroscope sensors during dynamic positioning is beneficial for detecting changes in the pitch and yaw angular velocities of the robot. When moving dynamically, the robot is in a stable condition if the gyroscope sensor output is a periodic signal seen using the autocorrelation function. Reducing the number of steps with the same trajectory, parameters, and servo duration speeds up the robot when going forward, but slows it down when sliding or rotating. The more step-motion, the smoother the servo angle change transition, and the lower the torque load, but the voltage decreases faster and requires more memory. The less step-motion, the quicker the servo angle change transition, and the greater the torque load, but the voltage declines slowly and requires less memory. Color detection is significantly impacted by ambient variables, hence it is required to recalibrate in varied situations.

VI. Acknowledgement

Thank you to the Electrical and Information Engineering Department, Engineering Faculty, Universitas Gadjah Mada for supporting this research.

REFERENCES

[1] C. N. Thai and M. Paulishen, “Using Robotis Bioloid Systems for Instructional Robotics,” pp. 300–306, 2011.

[2] J. A. Rojas-Quintero and M. C. Rodríguez-Liñán, “A literature review of sensor heads for humanoid robots,” *Rob Auton Syst*, vol. 143, 2021, doi: 10.1016/j.robot.2021.103834.

[3] S. Papadakis and V. Orfanakis, “The Combined Use of Lego Mindstorms NXT and App Inventor for Teaching Novice Programmers BT - Educational Robotics in the Makers Era,” in *International Conference EduRobotics 2016*, 2017.

[4] A. A. Shafie, “Geometrical Analysis on BIOLOID Humanoid System Standing on Single Leg,” no. May, pp. 17–19, 2011.

[5] A. Mohammed, L. Wang, and R. X. Gao, “Integrated image processing and path planning for robotic sketching,” in *Procedia CIRP*, 2013. doi: 10.1016/j.procir.2013.09.035.

[6] H. Hemami, F. C. Weimer, and S. H. Koozekanani, “Some Aspects of the Inverted Pendulum Problem for Modeling of Locomotion Systems,” *IEEE Trans Automat Contr*, vol. 18, no. 6, 1973, doi: 10.1109/TAC.1973.1100432.

[7] F. Gubina, H. Hemaml, and R. B. Mcghee, "On the Dynamic Stability of Biped Locomotion," *IEEE Trans Biomed Eng*, vol. BME-21, no. 2, 1974, doi: 10.1109/TBME.1974.324294.

[8] O. Tunçel, K. Altun, and B. Barshan, "Classifying human leg motions with uniaxial piezoelectric gyroscopes," *Sensors*, vol. 9, no. 11, 2009, doi: 10.3390/s91108508.

[9] W. Li, X. D. Yang, W. Zhang, and Y. Ren, "Modeling and Performance Investigation of a Piezoelectric Vibrating Gyroscope," *IEEE Sens J*, vol. 19, no. 21, 2019, doi: 10.1109/JSEN.2019.2930084.

[10] M. Bulatowicz *et al.*, "Laboratory search for a long-range T-odd, P-odd interaction from axionlike particles using dual-species nuclear magnetic resonance with polarized Xe129 and Xe131 Gas," *Phys Rev Lett*, vol. 111, no. 10, 2013, doi: 10.1103/PhysRevLett.111.102001.

[11] I. P. Prikhodko, B. Bearss, C. Merritt, J. Bergeron, and C. Blackmer, "Towards self-navigating cars using MEMS IMU: Challenges and opportunities," in *5th IEEE International Symposium on Inertial Sensors and Systems, INERTIAL 2018 - Proceedings*, 2018. doi: 10.1109/ISISS.2018.8358141.

[12] S. Dutta *et al.*, "Stability analysis of humanoid robots with gyro sensors subjected to external push forces," in *2019 2nd International Symposium on Devices, Circuits and Systems, ISDCS 2019 - Proceedings*, 2019. doi: 10.1109/ISDCS.2019.8719090.

[13] L. Hu, D. Navarro-Alarcon, A. Cherubini, M. Li, and L. Li, "On Radiation-Based Thermal Servoing: New Models, Controls, and Experiments," *IEEE Transactions on Robotics*, vol. 38, no. 3, 2022, doi: 10.1109/TRO.2021.3119399.

[14] C. L. Hwang and G. H. Liao, "Real-time pose imitation by mid-size humanoid robot with servo-cradle-head RGB-D vision system," *IEEE Trans Syst Man Cybern Syst*, vol. 49, no. 1, 2019, doi: 10.1109/TSMC.2017.2783947.

[15] K. Teachasrisaksakul, Z. Q. Zhang, G. Z. Yang, and B. Lo, "Imitation of dynamic walking with bsn for Humanoid robot," *IEEE J Biomed Health Inform*, vol. 19, no. 3, 2015, doi: 10.1109/JBHI.2015.2425221.

[16] J. H. Kim, "Multi-Axis Force-Torque Sensors for Measuring Zero-Moment Point in Humanoid Robots: A Review," *IEEE Sensors Journal*, vol. 20, no. 3. 2020. doi: 10.1109/JSEN.2019.2947719.